Feasibility Study of Utilizing Existing Infrared Array Cameras for Daylight Star Tracking on NASA's Ultra Long Duration Balloon (ULDB) Missions

Grant NAG5-8662

Summary of Research

For the period 15 July 1999 through 14 January 2004

Principal Investigator:

Dr. Giovanni G. Fazio

May 2004

Prepared for
NASA/Goddard Space Flight Center
Greenbelt, MD 20771-0001

Smithsonian Institution
Astrophysical Observatory
Cambridge, Massachusetts 02138-1596

The Smithsonian Astrophysical Observatory
is a member of the
Harvard-Smithsonian Center for Astrophysics

The Technical Officer for this grant is Dr. Jack Tueller, Code 661.0, NASA/Goddard Space Flight Center, Greenbelt, MD 20771-0001

ULTRA-LONG DURATION BALLOON (ULDB) FEASIBILITY STAR TRACKER STUDY

Giovanni G. Fazio
Volker Tolls

April 8, 2004

1. Introduction

The purpose of this study was to investigate the feasibility of developing a daytime star tracker for ULDB flights using a commercially available off-the-shelf infrared array camera. This report describes the system used for ground-based tests, the observations, the test results, and gives recommendations for continued development.

2. Test Setup

An overview of the test system is given in Fig. 1 and an actual picture is given in Fig. 2. The star tracker camera system consists of an Indigo Systems Merlin InGaAs Infrared camera. The camera is mounted on a Celestron tripod with a German equatorial mount (an azimuth-elevation mount would have been better by enabling easy sky-dips for background measurements). By using the mount hand controller, the camera could be moved manually in right ascension and declination, or, after setting up the controller, automatically by selecting an astronomical source stored in the hand controller.

The camera is connected to a computer via a serial data line for camera control and via a 12 bit parallel digital line for data acquisition. The digital data acquisition is performed using a BitFlow RoadRunner framegrabber card. The acquired data can either be displayed on-screen in real-time or stored on harddisc. Unfortunately, both operations cannot be performed simultaneously. But, the camera provides an analog NTSC compatible output signal which was connected to the computer monitor. The computer monitor was then operated in a picture-in-picture (PIP) mode allowing the simultaneous display of the analog video signal and the computer graphics output. This mode was essential for the first spatial calibration of the IR camera and for data acquisition since the camera frames could be seen in real-time.

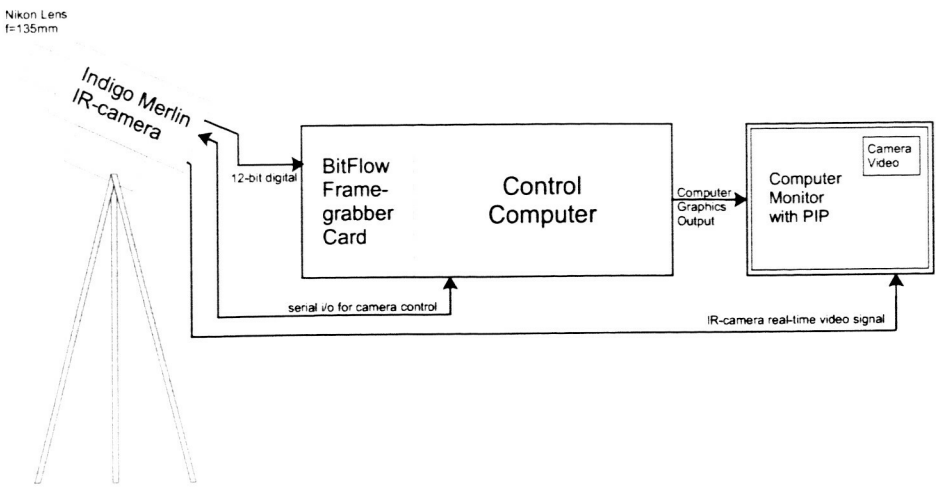

Figure 1: Star tracker camera test setup.

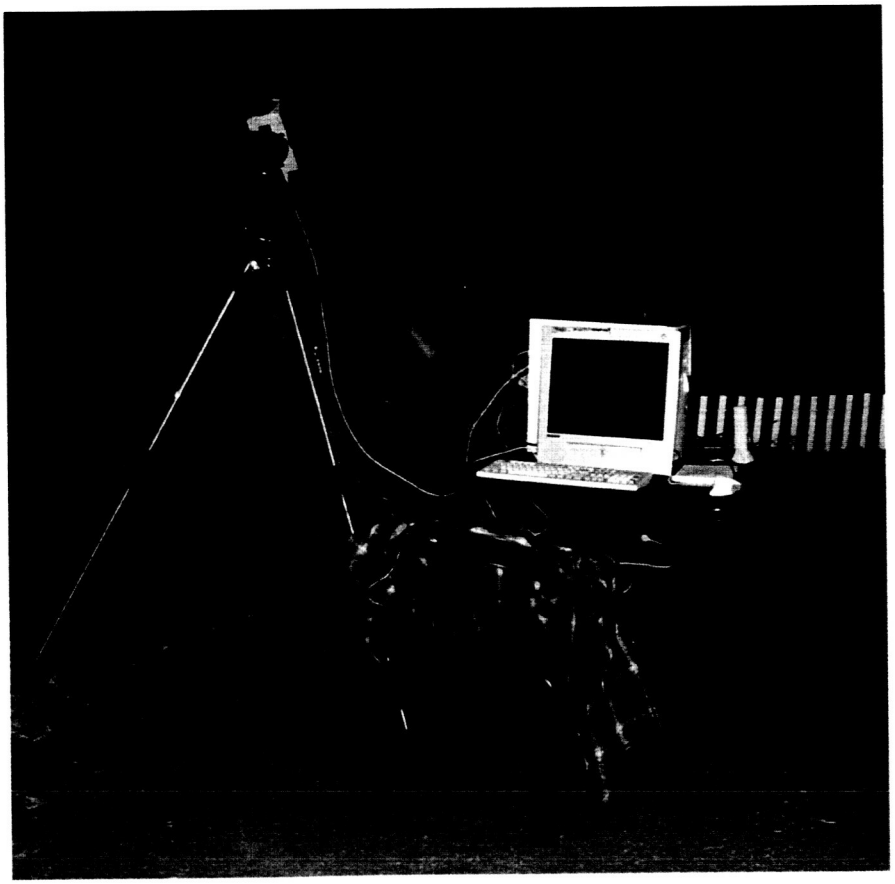

Figure 2: Star tracker camera test setup as "backyard astronomy".

3. Camera Specification

The camera used for this experiment was an Indigo Merlin camera with an InGaAs focal plane array (FPA) detector (ISC9809) with 320 x 240 pixels of 30 μm x 30 μm. The detector is sensitive in the wavelength range from 900 to 1680 nm. Figure 3 shows the spectral sensitivity as a function of wavelength and the locations of the infrared J- and the H-bands as used for the 2MASS-survey. The integration time used for all measurements was 16.6 msec. per frame. The detector was usually set to the high gain mode versus the low gain mode which requires more photons (thus stronger sources) to saturate the output signal. All other detector values were set to their default factory settings. The essential detector specifications are summarized in Table 1.

Table 1: Summary of detector specifications

Detector Type	InGaAs
Spectral Range	0.9 – 1.7 μm
Resolution	320 x 240
Pixel Size	30 x 30 μm
Well Capacity	170k e^- (high gain) 3.5M e^- (low gain)
Read Noise	< 70 e^- (high gain) < 700 e^- (low gain)
NEI (measured)	2.8 10^9 ph s^{-1} cm^{-2} (t=10ms, high gain) 5.8 10^9 ph s^{-1} cm^{-2} (t=16ms, low gain)
Non-Linearity	< +/- 0.5 %
Cross Talk	< 0.1 %
Integration Time	10 μs – 16.6 ms
Cooling	TE-stabilized
Digital Resolution	12 bit
Power	< 25 W

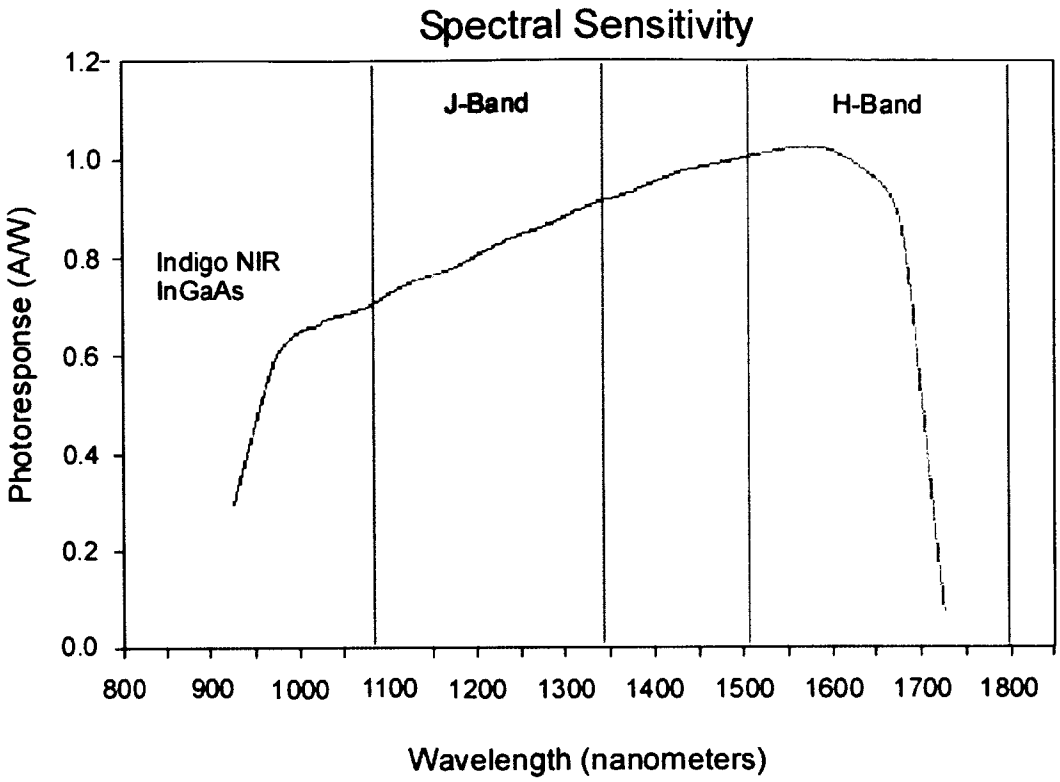

Figure 3: Spectral sensitivity of the Indigo Systems InGaAs near-IR detector. The J- and H-bands show the filter widths of the filters used for the 2MASS-survey (http://www.ipac.caltech.edu/2mass).

4. Software

The software used for this program consisted of a package called RRcapture, the program MerlinUI.exe from Indigo Systems, an IDL procedure called st_viewer, other IDL procedures for the analysis, and StarryNight Pro.

- The software package RRcapture was written by Ross Cutler and freely distributed on the WWW. However, the URL for downloading the program is no longer active. This program simplified the data acquisition from the camera using the BitFlow RoadRunner framegrabber interface. The acquired data are stored in a file.
- The program MerlinUI.exe is a GUI-based serial interface to control the operation of the Indigo Merlin camera via a serial connection. However, the program had some limitations such as not all camera functions could be controlled. The most important missing camera function was the switching of the detector gain mode. The switching had to be done using a terminal emulator program to interface to the camera. The program used here was Hyperterminal which comes with the Microsoft Windows operating system. Only one program, either MerlinUI or Hyperterminal, could be used at a time making the operation cumbersome. Rewriting the programs would have been too time consuming.

- The IDL procedure st_viewer is a widget-based program to read the acquired data and display them graphically. It can automatically average scans, subtract reference scans or baselines, correct for bad pixels, calculate the rms-noise in the images and calculate the integrated intensity in the measured sources as selected by the user. The measured signals can be visualized in a 3-dim. plot for closer inspection (see examples below). Finally, the analyzed data can be piped back to the main IDL program for further analysis by supplementary procedures.
- Starrynight Pro is an astronomical program for planning observations. It was used for an up-to-date view of the night sky to identify the good candidates for observation.

5. Observation

Because the camera is not background limited, the test observations from the ground at night are comparable to the conditions at the typical ULDB flight altitudes of 30 to 40 km. Initial estimates of the night background on the ground [e.g. measurements of the OH airglow and the thermal emission of the atmosphere, summary in Tokunaga 2000, which are assumed to be the dominant background signal source] and the day-time background at balloon altitude, extrapolated from Alexander et al. 1999, show that the number of background photons is negligibly small compared to the camera's inherent noise signal. Therefore, the conducted groundtests are immediately applicable for possible ULDB applications.

The data for the presented analysis were acquired on 12. December 2003 and 11. February 2004 between 8:00 pm and 12:30 am in Belmont, MA. The conditions were in both cases that cold-fronts had just moved through during the day leaving clear skies and low humidity. The temperature was about -1° C at the start of the observations and dropped to about -5° C at the end. The test setup was as described in §1. The camera was equipped with a f=135 mm Nikon photo-lens (largest aperture was 2.8). The observations were performed mainly looking towards the south with an elevation of 45° or higher. The observed sources were selected by their visual magnitude to be brighter than about 2 mag. Using the hand-controller, each source was manually centered in the cameras field of view (as described above, the source could by identified on-screen in the video signal display). Then, between 20 and 200 frames (the resulting integration time was between 0.332 and 3.32 seconds) were acquired, the camera lens was covered, and the same number of frames was acquired as reference signal. In order to get a result that is independent of the location of the signal on the detector, a second measurement was performed positioning the source on a second location on the detector. The positioning was not exactly on the same pixels for each measurement, but within +/- 30 pixel vicinity. The measured intensities ranged from about 20 counts to 3300 counts. The peak counts, including camera background signal, in 2 pixels of the brightest source, Betelgeuse, were 4096 counts, the maximum of the 12 bit A/D converter in the camera. However, the saturation level was only violated slightly such that the result still agrees very well with all other measurements (see 6. Results). The RMS noise (after background

subtraction) was about 2.0±0.3 counts for 1.66 sec integration time and about 1.4±0.2 counts for 4.98 sec integration time. These values should be considered an upper limit because we did not perform a gain calibration. The gain might vary slightly from pixel to pixel and, thus, increasing the noise slightly. However, within its error it decreases with $1/\sqrt{t_{\text{int}}}$. For the 1.66 sec integration measurement, the resulting signal-to-noise ratio was about 20 for a 4.8 mag star (the peak intensity was about 30 counts).

6. Results

Since the sources observed in December were observed again in February, the analysis concentrated on the measurements from the February observing run. A total of 17 fields were observed. Each field was observed twice with slightly offset centers such that the observed sources were located in different pixels. Figure 4 shows the result of the field centered on Alnilam (α = 5h 36m 12.8s, δ = -1° 12' 6.9"). Eight IR sources could be identified in this field of 4° x 3° size. However, the source located in the last column of the array was not included in the analysis since the intensity could not be determined correctly, and another source was excluded which was observed with a much lower intensity than expected from the 2Mass catalog (about 1000 counts were expected, but the observation showed only 40 and 110 counts in the two measurements). The identification of all sources in this field was performed by determining their position in the field, the pixel with the largest intensity, calculating the distances to all adjacent sources, comparing these measured distances to the distances calculated from the source positions in the 2Mass catalog, and using the expected intensities as given in the J-band results of the 2Mass catalog as verification. The same analysis was performed on each of the 34 observations. In general, distances from the measured star fields agreed with the 2Mass distances to the sub-pixel level (FOV_{pixel} = 45.8" calculated, = 45.32" derived from the star fields). This agreement can be improved by fitting point spread functions to the measured intensities.

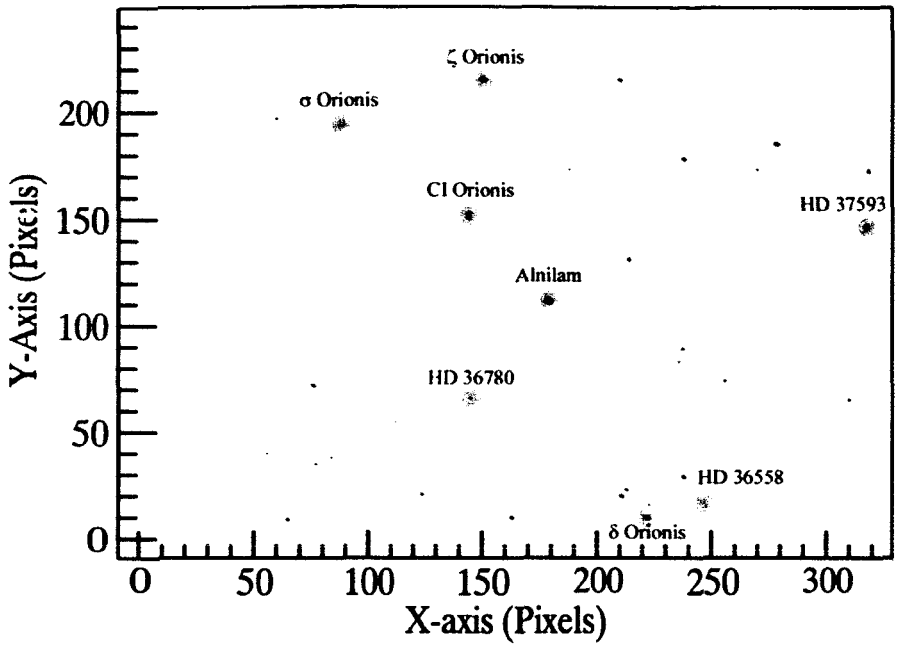

Figure 4: Star tracker camera result of the Alnilam field (α = 5h 36m 12.8s, δ = -1° 12' 6.9"). The circled sources were identified; all other black spots are array artifacts like hot pixels.

The response from each observed star, Figure 5 shows the result for Beutelgeuse, was derived by summing the pixel response of all pixels within concentric rings centered at the largest response (thus, deriving the integrated intensity). Typically, the radius of these rings was only 2 to 3 pixels. Then, the sum was corrected for the background signal by calculating the mean of the pixels surrounding the star and subtracting it from the integrated intensity. Figure 6 summarizes the results in the camera calibration plot. Shown are J-band magnitude (top plot) and the H-band magnitude (bottom plot) versus the integrated intensity for each observed star (3 stars with doubtful integrated intensities have been excluded). The J-band and h-band magnitudes were taken from the 2MASS survey. The dotted line in each plot shows a linear fit to the data points.

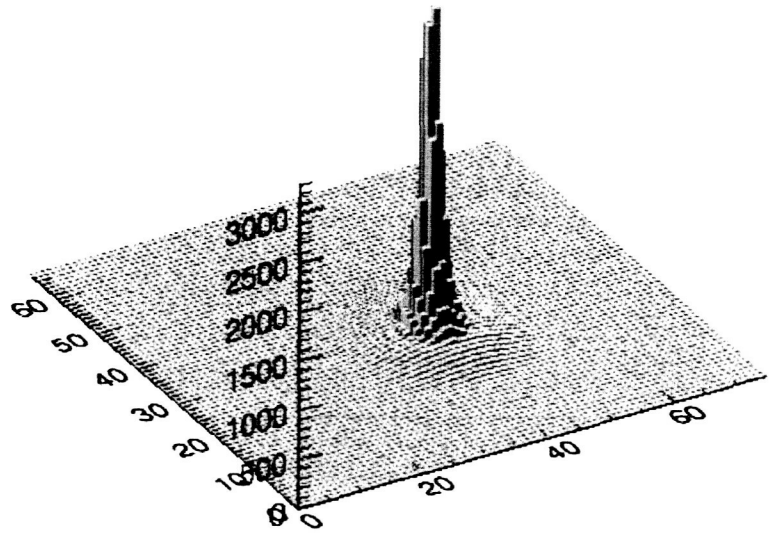

Figure 5: Observation of Betelgeuse (α = 5h 55m 10.3s, δ = +7° 24' 25.3"), the star with the strongest emission observed.

As expected, the measurements follow the J-band intensities better than the H-band intensities because the J-band sits in the middle of the wavelength range where the detector is sensitive whereas the H-band is only partly covered. The result is even more remarkable since no gain adjustment has been performed such that all pixels of the array have the same gain. The camera is equipped with a gain adjustment with factory values which was turned off for the measurements. Further observations would be required to characterize the effects of this adjustment. An independent gain calibration with known laboratory calibration sources would be one of the next steps in the development of a star tracker. Overall, the Indigo Merlin IR camera has performed very well during these tests considering that it was designed for applications such as IR vision support for firefighters and similar applications, but not for astronomy. The next chapter summarizes next steps for further development of a star tracker.

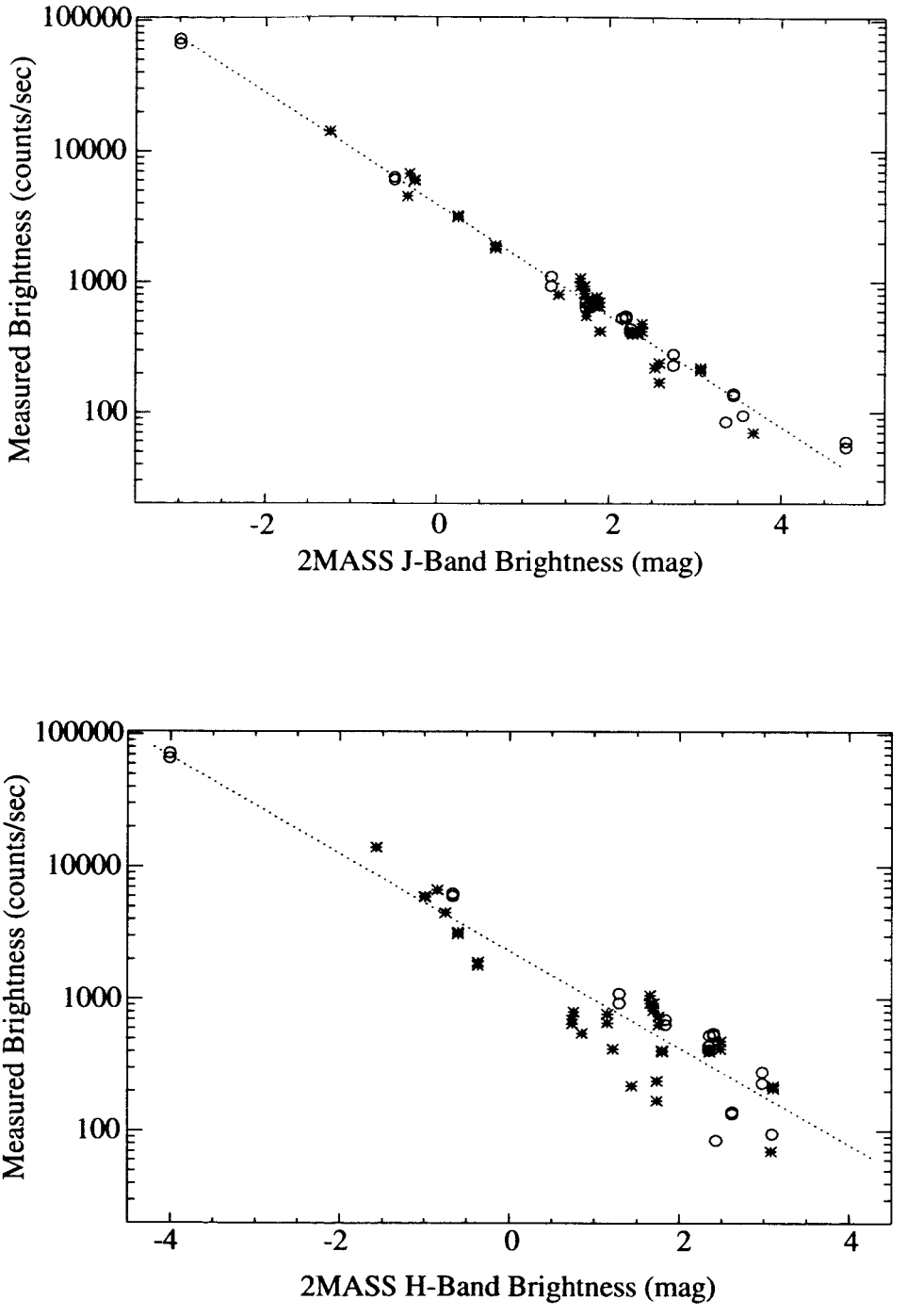

Figure 6: J-band magnitude (top plot) and H-band magnitude (bottom plot) versus the observed integrated star intensities. The J-band magnitudes match the observed intensities much better than the H-band magnitudes. Data points marked with open circles were taken with 1.66 sec integration time and data points marked with asterisks were taken with 4.98 sec integration time. The result of this analysis can be found in a table with auxiliary information in Attachment 1.

7. Outlook

The results were based on using a commercial IR camera as a star tracker. More testing and evaluation should be performed on newer generation IR cameras. The main disadvantages of the camera used were:

	Current limitation	Future solution
1	Limited array size with 320 by 240 pixels.	New generation of IR cameras have larger arrays, e.g. Indigo Phoenix camera series has the option of a 640 by 480 pixel NIR-array.
2	Longest integration time per frame is 16.6 msec. corresponding to a single NTSC frame.	Possible custom camera software might overcome this problem.
3	Digital resolution is only 12 bits.	The already mentioned Phoenix camera series has 14 bit resolution. 16 bit would actually be preferred. It needs to be investigated if it is possible with external A/D converter.
4	The used lens was a Nikon 135 mm lens designed for photography in the visible part of the spectrum, but not optimized for use in the NIR.	The search to identify manufacturer for NIR lenses needs to be identified. The only known lens manufacturer is a Italian company whose US distributor went out of business in early 2003.
5	No band limiting filters were used.	Evaluation of results using band limiting filters such as a J-Band filter. However, this will reduce the number of measured photons and therefore might limit the sensitivity too much.

Further activities to be considered for continued development would include:

1. Evaluate the performance and availability of the latest technology, e.g. cameras with larger arrays and higher sensitivity.
2. Build a stand-alone star tracker consisting of a camera and a control computer that can be flown piggy-back on a balloon flight to initially test its observing characteristics and later as a secondary guidance system.
3. Create a star reference catalog tailored for the developed camera system.
4. Develop analysis software that takes the point-spread function into account, improving the spatial resolution of the system to a sub-pixel level.
5. Develop software for the stand-alone system for the control of the camera, the data acquisition, and the data analysis. Currently data analysis requires human

interaction which is not possible during a balloon flight. Software that was written for the testing above could be used as a starting point. For the first test flights, this software doe not necessarily need to perform a complete analysis (star recognition star position calculation and pointing determination), it might be sufficient to store the recorded data on-board. This would enable a faster in-flight performance testing of the camera regarding sensitivity and background.

6. Conduct balloon test flights as a back-up system.
7. Analyze and evaluate the data.
8. Study improvements for the existing camera system.

8. Summary

The current simple commercial version of the near-IR camera used as star tracker performed very well at ground level. With a simple test setup we could measure and identify stars from -3 mag down to 4.5 mag (J-band). The response of the camera was surprisingly very linear when plotting the logarithm of the measured brightness versus the J-band brightness from the 2MASS catalog. The camera performed during these tests according to its specifications. However, the capabilities of the camera were limited by its sensitivity and array size (320 by 240 pixels). Future generation of cameras will overcome these limitations. Cameras with larger arrays (640 by 480 pixels) and slightly improved sensitivity are already available (e.g. Indigo Systems SU640-1.7RT camera) enabling the development of a full star tracker camera in near future.

9. Acknowledgement

This publication makes use of data products from the Two Micron All Sky Survey, which is a joint project of the University of Massachusetts and the Infrared Processing and Analysis Center/California Institute of Technology, funded by the National Aeronautics and Space Administration and the National Science Foundation.

10. References

Alexander, C.D., Swift, W., Ghosh, K., and Ramsey, B., SPIE Vol. 3779, 47-54, 1999

Indigo System, Calibration Data for Merlin NIR camera, 2000

Tokunaga, A.T. in "Allen's Astrophysical Quantities", ed. Cox, A.N., Springer Verlag, 2000

Table 2: Observed sources and results of analysed fields

Name	SAO #	File	Frames	R.A. h	m	s	Dec. deg	m	s	Mag	Spectral	j_m	j_cmsig	h_m	h_cmsig	k_m	k_cmsig	Position	counts	err_counts	rms	mean
Bellatrix	112740	20040211_s001.dat	100fr	5	25	7.86820	6	20	59.0442	1.64	B2III	2.149	0.282	2.357	0.168	2.375	0.256	178,107	530	20	1.90	10.68
		20040211_s002.dat	100fr															159,97	530	20	1.88	10.96
Alnilam	132346	20040211_s003.dat	100fr	5	36	12.81257	-1	12	6.9021	1.69	B0Ia	2.191	0.324	2.408	0.18	2.273	0.282	179,111	550	40	1.89	12.86
																		151,215	440	20		
																		222,10	280	15		
																		146,77	135	10		
		20040211_s004.dat	100fr															89,193	60	10		
																		213,111	530	20	1.95	12.85
																		184,215	410	20		
																		256,10	230	20		
																		180,77	140	20		
																		180,152	110	20		
																		123,193	54	10		
Procyon	115756	20040211_s005.dat	100fr	7	39	18.53807	5	13	39.0276	0.4	F5IV-V	-0.498	0.15	-0.666	0.27	-0.658	0.322	155,131	6300	200	2.10	8.42
		20040211_s006.dat	100fr															182,142	6000	200	2.08	8.80
Alhena	95912	20040211_s007.dat	100fr	6	37	42.70234	16	23	57.8934	1.93	A0IV	1.729	0.244	1.836	0.202	1.917	0.22	162,158	700	40	1.84	8.96
		20040211_s008.dat	100fr															139,159	640	40	1.85	8.40
Betelgeuse	113271	20040211_s009.dat	100fr	5	55	10.28919	7	24	25.3308	0.45	M2Ib	-2.989	0.102	-4.007	0.162	-4.378	0.186	149,120	72000	2000	5.47	11.76
		20040211_s010.dat	100fr															183,134	66000	2000	5.12	10.02
Castor	60179	20040211_s011.dat	100fr	7	34	36.00456	31	53	19.0912	1.58	A2Vm	1.33	0.266	1.292	0.152	1.229	0.24	149,129	930	50	1.86	6.89
		20040211_s012.dat	100fr															209,159	1100	100	1.84	6.83
																		139,182	95	5		
Pollux	79666	20040211_s013.dat	300fr	7	45	19.36383	28	1	34.7171	1.16	K0IIIvar	-0.315	0.232	-0.845	0.178	-0.936	0.16	183,130	6700	300	1.73	8.01
																		245,85	400	20		
		20040211_s014.dat	300fr															4,135	170	20		
																		199,145	6700	300	1.64	8.45
																		261,100	410	20		
																		20,151	240	30		
Capella	40186	20040211_s015.dat	300fr	5	16	41.29564	45	59	56.5054	0.08	M1: comp	-1.249	0.202	-1.573	0.184	-1.735	0.144	163,123	14000	500	1.95	8.68
		20040211_s016.dat	300fr															194,145	14000	500	2.32	13.45
Menkalinan	40750	20040211_s017.dat	300fr	5	59	31.76943	44	56	50.7657	1.9	A2V	1.756	0.222	1.76	0.168	1.778	0.19	31,94	220	40		
																		231,119	3200	100	1.55	7.95
																		180,110	700	40		
		20040211_s018.dat	300fr															167,165	640	30		
																		269,134	3100	200	1.50	8.26
																		218,126	650	40		
																		206,180	740	40		
Regulus	98967	20040211_s019.dat	300fr	10	8	22.45938	11	58	1.9025	1.36	B7V	1.665	0.314	1.658	0.186	1.64	0.212	207,164	930	40	2.10	11.01
		20040211_s020.dat	300fr															156,132	1070	50	1.46	9.65
																		307,169	420	20		
Alphard	136871	20040211_s021.dat	300fr	9	27	35.25182	-8	39	31.2601	1.99	K3III	-0.256	0.146	-0.99	0.192	-1.127	0.208	152,142	5900	300	1.91	12.17
		20040211_s022.dat	300fr															192,158	6000	300	1.91	11.43
Theta Hydrae	117527	20040211_s023.dat	300fr	9	14	21.79327	2	18	54.0872	3.89	B9.5V	3.455	0.182	4.04	0.013	3.943	0.005	186,231	800	40	1.37	8.94
		20040211_s024.dat	300fr																			
Gomeisa	115456	20040211_s025.dat	300fr	7	27	9.07229	8	17	21.8721	2.89	B8Vvar	3.061	0.294	3.109	0.234	3.101	0.264	250,114	660	40	1.37	8.20
																		223,212	550	40		
		20040211_s026.dat	300fr															196,106	210	25		
																		247,158	770	50	1.39	7.67
																		193,150	220	20		
Merak	27876	20040211_s027.dat	300fr	11	1	50.39076	56	22	56.4412	2.34	A1V	2.269	0.244	2.359	0.164	2.285	0.244	157,141	420	30	1.41	7.81
																		52,195	70	20		
		20040211_s028.dat	300fr															61,137	400	20	1.37	7.74
Dubhe	15384	20040211_s029.dat	300fr	11	3	43.83688	61	45	4.0280	1.81	F7V	-0.34	0.21	-0.751	0.144	-0.829	0.17	152,132	4500	200	1.60	7.36
		20040211_s030.dat	300fr															176,145	4500	200	1.83	7.96
Phecda	28179	20040211_s031.dat	300fr	11	53	49.74129	53	41	41.0387	2.41	A0V SB	2.381	0.29	2.487	0.174	2.429	0.288	142,135	420	20	1.43	8.64
		20040211_s032.dat	300fr															165,127	480	40	1.37	9.73
Alioth	28553	20040211_s033.dat	300fr	12	54	1.63298	55	57	35.4348	1.76	A0P	1.713	0.246	1.698	0.186	1.625	0.266	151,127	820	40	1.79	9.86
																		32,220	1800	100		
		20040211_s034.dat	300fr															186,132	930	50	1.69	9.46
																		66,225	1900	100		